Polymer Microparticles Exhibit Size and Shape Dependent Accumulation around the Nucleus after Endocytosis

*Poornima Kolhar and Samir Mitragotri**

Particulate drug delivery has received significant attention in the last few decades. The effect of particle properties such as size, shape and surface properties on particle-cell interaction has been studied. Here, intracellular accumulation and subsequent spatial segregation of spherical and rod shaped microparticles is investigated. It is observed that both spherical and rod shaped particles exhibit perinuclear accumulation. However, when the cells are fed with binary mixtures of particles, they spatially segregate in the cytoplasm based on their shape and size. Larger particles exhibit preferential accumulation closer to the nucleus. These results have potential implications in understanding the biophysical forces operating in the cells that impact the intracellular organization of drug carriers as well as organelles.

1. Introduction

The intracellular compartment is a highly organized environment consisting of various organelles and ingested foreign bodies such as microorganisms or particles. The organelles inside the cell possess various sizes and shapes, for example, mitochondria which possess a rod-like shape[1] and endosomes which are generally spherical in shape.[2] These organelles traverse the cytoplasm via microtubule-based transport and are organized in the cell depending on their transport properties as well as intra-organelle interactions.[2–4] Organization of intracellular organelles has been a topic of fundamental interest to cell biology. Organelle organization, especially of endosomes, has also been of high significance to drug delivery.[5,6] Particulate drug delivery carriers are generally internalized by cells through endocytosis and are trafficked on microtubules. Transport and eventual distribution of endosomes in cells has a significant impact on the effectiveness of drug delivery methods.[7]

Distribution of cellular organelles as well as endocytosed foreign materials is governed by their transport properties on microtubular and actin network.[4,8] In fact, such distribution is actively managed by melanophores in fish and frogs to regulate skin color for camoflouge.[9] From a fundamental perspective, three key parameters dictate the distribution of objects within cells; (i) the transport properties, which determine the rate at which the objects are carried towards or away from the nucleus on microtubules. Such transport is usually symmetric and birdirectional, thus randomizing the likelihood of particle motion,[2] (ii) aggregation and clustering of endosomes and lysosomes upon close approach, which is often governed by proteins such as Rab7 that accumulate on the surface of endosomes[10] and (iii) spatial confinement imposed by the cell geometry, which includes increased thickness of cells around the nucleus compared to that near the cell boundary due to spreading of cells on the substrate.[11] Collectively, these factors make particle distribution within the cells a complex phenomenon that depends on the interplay between transport properties, kinetics of endosome fusion and geometric confinement. Such phenomena are also widely common in non-biological field and have found wide interest in the scientific community. Some of the examples include coffee stains,[12] powder compacting,[13] DNA-RNA microarray deposition[14] and patterning for electronics applications[15]

Various studies have reported intracellular distribution of particles after endocytosis.[16,17] These include studies focused on mechanisms of internalization, intracellular trafficking and eventual localization of particles within the cells.[18–21] Relatively few studies focus on assessing intracellular distribution after feeding different types of particles to cells. One study has reported that cells can induce spatial segregation of particles based on their size.[22] Specifically, cells, when fed with a mixture of 1 μm and 3 μm microspheres, exhibited preferential accumulation of larger particles near the nucleus. The mechanisms responsible for this segregation, however, are not clear. Since many particle parameters including diameter, surface area and volume were different for 1 and 3 μm spheres, it is not clear if any of these parameters play a prominent role in segregation. Here, we address this challenge by preparing particles of various shapes and sizes and assessing their accumulation and subsequent organization in the cells. Particles shape has been extensively researched in the context of drug delivery. Shape of the particles has been shown to impact a number processes involved in particle cell interactions, such

P. Kolhar
Biomolecular Science and Engineering
University of California
Santa Barbara, CA 93106, USA
Prof. S. Mitragotri
Department of Chemical Engineering
University of California
Santa Barbara, CA 93106, USA
E-mail: samir@engineering.ucsb.edu

DOI: 10.1002/adfm.201102918

as phagocytosis,[23,24] endocytosis[17,19] and *in vivo* delivery.[25–27] Here, we explore the possible implication of shape in intracellular particle accumulation.

2. Experimental Section

Cell culture: Human umbilical cord endothelial cells were purchased from ATCC, Manassas, VA, USA. The cells were cultured in Medium 200 along with 1× low serum growth supplement (LSGS; Invitrogen, Carlsbad, CA, USA). Cells were grown under standard culture conditions (37 °C and 5% CO_2).

Synthesis of non-spherical particles: Amine-modified polystyrene spheres of different sizes (1 μm, 3 μm, 6 μm) were purchased from Polysciences (Warrington, PA, USA). Rod-shaped particles were prepared by physically stretching the spheres using the film stretching method described in Champion *et al*.[28] The particles were added to 10% polyvinyl alcohol solution (hot water soluble, Mol. Wt. 80–100 kDa, Sigma-Aldrich, St Louis, MO, USA) along with 2% (w/v) glycerol, which acts as a plasticizer. 50 ml of this mixture was dried overnight to form a film on a custom-made tray (19 cm × 23 cm). 5 cm × 5 cm pieces of the dried film were mounted on a custom-made axial stretcher. The film was then stretched in mineral oil at 120 °C at the rate of 0.3–0.5 mm/s. The film was allowed to cool and then immersed in isopropanol overnight to remove mineral oil. The films were then dissolved in 15% isopropanol and heated to 70 °C to recover the particles. The particles were washed 8 times in 15% isopropanol with 15 minute heating at 70 °C prior to centrifugation. The particles were finally suspended in water. For scanning electron microscopy, particles were coated with Gold (Hummer 6.2 Sputtering System; Anatech Ltd., Union City, CA, USA) and imaged with Sirion 400 scanning electron microscope (FEI Co., Hillsboro, OR, USA) at 3 eV.

Fluorescent tagging of the particles: The particles were incubated with 1 mg/mL NHS Rhodamine or NHS 5-Fam (Sigma-Aldrich, St Louis, MO, USA) in PBS for 3 h. The particles were then washed with PBS to remove the excess dye.

Segregation experiment: Endothelial cells were allowed to attach to a glass cover slip and incubated with particles for various time points. When particles of varied sizes/shapes were incubated with the cells, the total volume of particles was maintained constant. Internalization of particles was analyzed by imaging the cells using an inverted confocal microscope Olympus Fluoview 500 (Olympus America Inc., Center Valley, PA, USA). To assess the role of microtubule transport, cells were incubated with 0.3 μM Nocodazole in some experiments and the segregation experiment was performed for 6 h.

Segregation potential analysis: Confocal micrographs of cells incubated with particles were obtained. The images were analyzed using Image J software. The fluorescent images were thresholded to count the particles. The fluorescence for a region directly correlates with the number of particles in that region. The dimensions of the nucleus (a [major axis], b [minor axis]) were estimated and an elliptical region was drawn with major axis 1.5a and minor axis 1.5b around the same center. The ratio of particles of type 1 in the above mentioned region to the total number of particles in the cell, ${P_1}^N$, was estimated as a ratio of the red fluorescence in the region to the total red fluorescence in the whole cell. Similar analysis was done to the green fluorescent image and the ratio for type 2 particles, ${P_2}^N$, was estimated. The segregation potential between particles of type 1 and type 2, $S_{1\text{-}2}$ was calculated as described below.

$$S_{1-2} = \frac{{P_1}^N}{{P_2}^N}$$

3. Results and Discussion

Spherical polystyrene particles of various sizes (1 μm and 3 μm) were stretched to form rods using the film stretching method.[23] Particles were fluorescently labeled as described in methods. The particles were fed to endothelial cells and perinuclear accumulation[29] of particles was monitored over a period of time. When cells were exposed to a mixture of 1 μm and 3 μm spheres for 72 h, higher perinuclear accumulation of 3 μm spheres was observed compared to that of 1 μm spheres (**Figure 1**a). However, when cells were exposed to a mixture of 3 μm spheres and the rods stretched form these spheres (8.75 μm × 1.5 μm × 1.5 μm), clear separation of particles was observed with 3 μm spheres accumulating closer to the nucleus (Figure 1b). Extent of segregation of particles, *S*, in the perinuclear region was calculated as the percent of the two types of particles in the perinuclear region as defined in methods. $S_{1-2} > 1$ indicates segregation of particles so that type 1 particles are closer to the nucleus and vice versa whereas $S_{1-2} = 1$ indicates no segregation. The average segregation S_{1-2} for spheres of diameters 3 μm and 1 μm is 1.5 (where, 1 corresponds to 3μm and 2 corresponds to 1 μm, Figure 1c) indicating higher perinuclear accumulation of 3 μm spheres compared to 1 μm spheres.

Various combinations of sizes and shapes of particles were fed to cells and their segregation was measured (**Table 1**; **Figure 2**). High segregation was observed between 3 μm spheres and rods of 8.75 μm length and 1.5 μm diameter. Both particles had identical total volumes but the spheres exhibited significant perinuclear accumulation compared to rods. High segregation was also found in case of 3 μm spheres and relatively low-aspect ratio rods (4.83 μm ×2 .33 μm; Figure 2a), indicating that the aspect ratio of the particles does not play a major role in segregation.

No segregation was found between 1 μm spheres and rods stretched from them (Figure 2c). This observation is in stark contrast to that observed for 3 μm particles, where the same aspect ratio of rods was adequate to induce segregation. In another peculiar example, rods stretched from 1 μm spheres and 3 μm spheres with comparable aspect ratios did not exhibit segregation (Figure 2b).

The segregation of the particles by the cells can be seen as early as 24 h (**Figure 3**). In order to investigate whether the observed segregation was a result of difference in the rate of internalization or intracellular transport, the cells were first incubated with 1 μm spheres, which otherwise localize away form the nucleus compared to 3 μm spheres (**Figure 4**a) or rods stretched from 3 μm spheres, which otherwise localize away

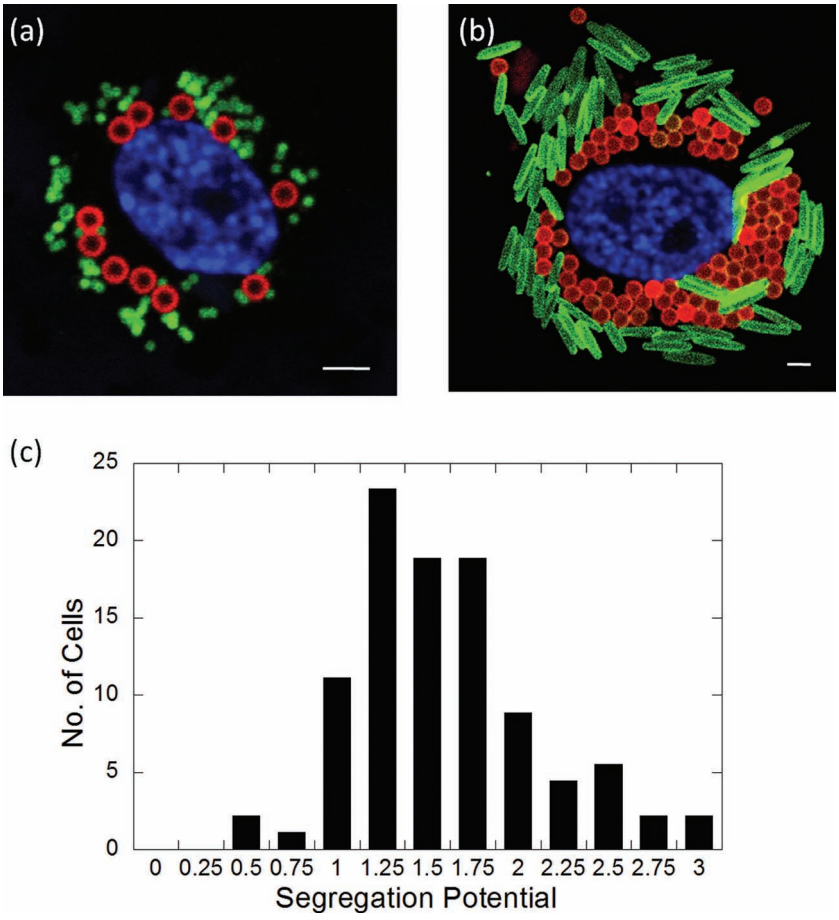

Figure 1. Segregation of particles by cells. (a) Confocal micrograph showing 1 μm spheres in green, 3 μm spheres in red internalized by HUVEC cells. Nucleus is stained blue with Dapi. (b) Confocal micrograph showing rods in green, 3 μm spheres in red and nucleus stained blue with Dapi. (c) A plot of distribution frequency of segregation potentials over a population of cells. Scale bar: 6 μm.

from the nucleus in the presence of 3 μm spheres (Figure 4c). These particles, when incubated with cells by themselves, exhibited perinuclear accumulation (Figures 4a,c). However, when 3 μm spheres were added to these cells 24 h later, they displaced the 1 μm spheres (Figure 4b) as well as the rods (Figure 4d) and preferentially accumulated in the perinuclear region. These results indicate that the segregation of particles in the cells does not originate from the difference in the rate of internalization of the particles but from the intrinsic properties of cells and/or particles.

Table 1. Summary of particle segregation.

P1	P2	S_{1-2}
3 μm spheres	1 μm spheres	1.5 ± 0.01
3 μm spheres	Rods, 8.75 μm × 1.5 μm	3.7 ± 0.15
3 μm spheres	Rods, 4.83 μm × 2.33 μm	3.18 ± 0.17
1 μm spheres	Rods, 3.89 μm × 0.51 μm	~1
Rods, 4.83 μm × 2.33 μm	Rods, 8.75 μm × 1.5 μm	~1
Rods, 8.75 μm × 1.5 μm	Rods, 3.89 μm × 0.51 μm	~1
6 μm spheres	3 μm spheres	2.7 ± 0.20
3 μm spheres	0.5 μm spheres	2.3 ± 0.5
3 μm spheres	0.1 μm spheres	~1

The 3 μm spheres and the rods stretched from 3 μm spheres do not differ in mass or volume. Hence, volume of the particle is not the primary determinant of segregation. Further, the data in Table 1 indicate that the aspect ratio of particles is also not a factor in segregation. Size of the particles, on the other hand, appears to play a significant role. Although various possible mechanisms may explain particle segregation, it is likely that the preferential segregation of the 3 μm spheres near the nucleus originates from the differences in the cell thickness near and away from the nucleus. Specifically, the cells, those used in this study and several others, exhibit extensive spreading on the substrate and exhibit higher thickness of the cytoplasm near the nucleus compared to that away from the nucleus. The thickness of the nucleus was found to be approximately 4 μm by confocal microscopy (**Figure 5**a). The nucleus creates a wedge-shaped area inside the cells that provides space for accumulation of particles and allows preferential accumulation of larger particles near the nucleus. Also the bidirectional motion of the particles on the microtubules facilitates transport of particles towards the perinuclear region and may in fact help increase the packing efficiency of the particles in the cells similar to the effect seen when powders are agitated to separate based on size and shape of the particles.[30,31] Microtubules clearly played a role in observed perinuclear accumulation and segregation since seggregation was lost when the microtubule structure is disrupted by exposure of cells to nocodazole (Figure 5b, c).

The seggregation phenomenon is likely to manifest prominently when the length scale of the particles is comparable to the height of the cytoplasm near the nucleus. 1 μm spheres and rods stretched from them (width = 0.5 ± 0.12 μm) as well as rods with widths 1.5 ± 0.12 and 2.0 ± 0.12 did not exhibit segregation in spite of the differences in their height. However, 3 μm spheres and rods stretched from 3 μm spheres exhibited high segregation. It appears that the threshold dimension for segregation is 3 μm in height.

To further explore the threshold dimension, experiments were performed with spherical particles of various diameters. 0.1 μm, 0.5 μm, and 6 μm diameter particles were used along with the previously described 3 μm particles (**Figure 6**). In all the conditions, where the second particle has a diameter lower than 3 μm, the 3 μm particles segregate into the perinuclear region. However, 6 μm spheres accumulate closer to

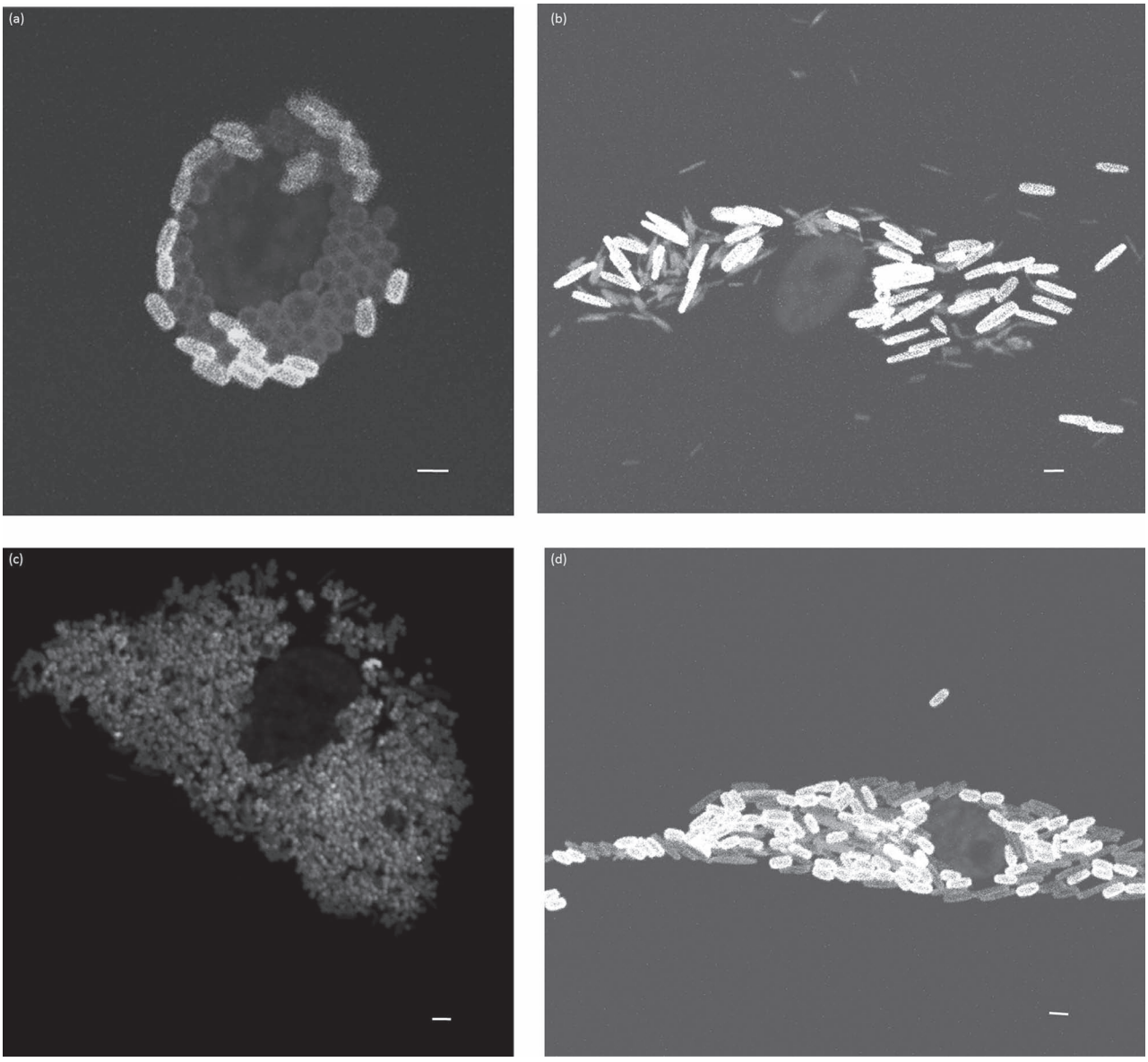

Figure 2. Intracellular accumulations of various particle combinations. Confocal micrographs of cellular accumulation of (a) 3 μm spheres in red and rods (4.83 μm × 2.33 μm) stretched from the 3 μm spheres in green (b) Rods (3.89 μm × 0.51 μm) stretched from 1 μm spheres in red and rods (8.75 μm × 1.5 μm) stretched from 3 μm spheres in green (c) rods (3.89 μm × 0.51 μm) stretched from 1 μm spheres in red and 1 μm spheres in green (d) Rods stretched from 3 μm with dimensions 4.83 μm × 2.33 μm in green and rods with dimensions 8.75 μm × 1.5 μm in red. Scale bar: 4 μm.

the nucleus compared to 3 μm. These results conclusively show that the threshold radius for segregation is around 3 μm and when the particle height is equal to or higher than 3 μm there is segregation into the perinuclear region while any diameter lower than 3 μm shows no segregation. Steric hindrance offered by accumulation of larger particles close to the nucleus also seems to play a role. Specifically, when cells were fed with a mixture of 3 μm and 0.1 μm particles, no segregation was observed, that is, smaller particles seem to distribute throughout the perinuclear region and exhibit no segregation. This suggests that 0.1 μm particles may be able traverse through the dense packing of larger particles and approach the nucleus.

Previous studies have demonstrated that mixtures of spherical particles are spatially segregated within cells by size, with larger spheres located closer to the nucleus and the smaller particles arranged along the periphery of the larger particles.[22] Experiments reported here with mixtures of particles possessing different shapes reveal that the observed segregation is likely to originate from height of the particle rather than the volume of the particle and at least one of the particles should have a height above 3 μm. This specific limit may in turn depend on the cell type due to differences in the cell heights depending on their type. Although particle segregation is an intrinsic property of cells, varying physical properties of particles such as shape and size can control the extent and the order of segregation. Further

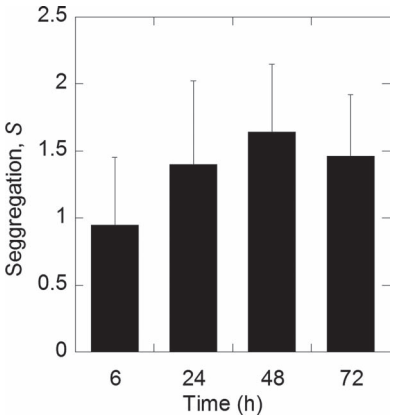

Figure 3. Time course of particle segregation. Bar graph showing the average segregation potential plotted as a function of time for a particle mixtures consisting of 1 μm spheres and 3 μm spheres.

experiments with various polymeric particles can unfold the role of chemical and mechanical properties, which may also potentially influence the segregation within cells.

The results presented here have implications for understanding the localization of cellular organelles. Most intracellular organelles are relatively small and may not be limited by spatial constraints in terms of their localization. However, certain organelles, for example, mitochondria can possess large dimensions (several microns), which may make them susceptible to the phenomenon reported here. Note also that the critical dimension of 3 μm may be potentially reduced for small cells or those that exhibit extensive spreading. Particles

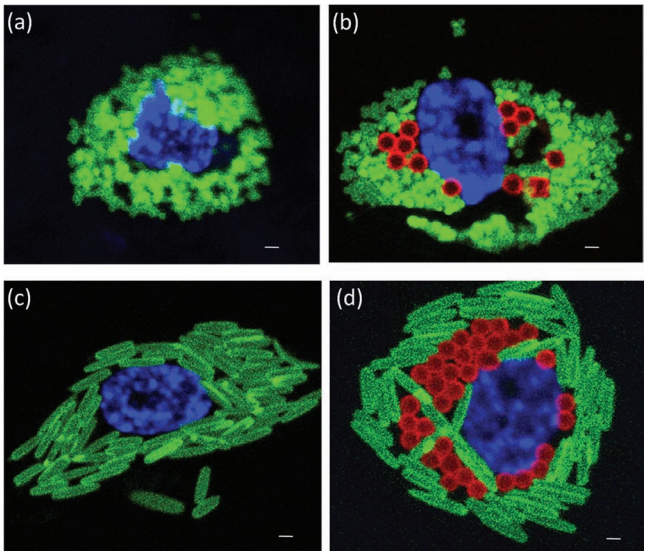

Figure 4. Mechanistic study of intracellular segregation. Confocal micrograph showing intracellular accumulation of (a) rods (8.75 μm × 1.5 μm), (c) 1 μm spheres in green. After 24 h the cells were further incubated with 3 μm spheres. (b) Confocal micrographs showing accumulation of 3 μm spheres (red) and rods (8.75 μm × 1.5 μm) in green.(d) Confocal micrographs showing accumulation of 3 μm spheres (red) and 1 μm spheres (green). The nuclei in the micrographs appear blue. Scale bar: 3 μm.

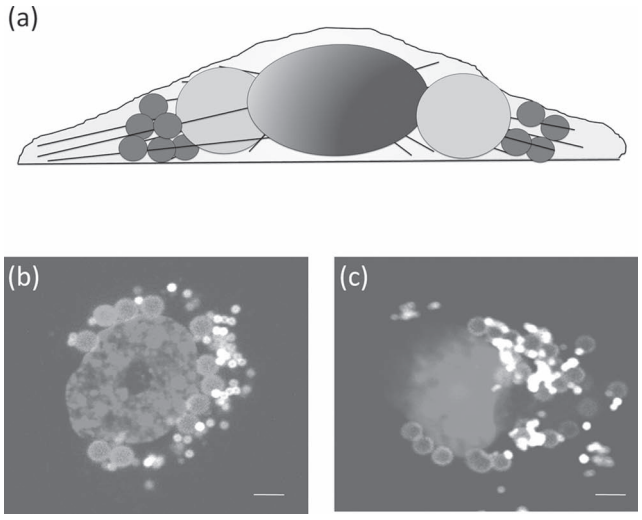

Figure 5. Cellular factors responsible for segregation effect. (a) Schematic of the cell showing the wedge shape due to the nucleus and accumulation of particles around the nucleus based on size. The particles are transported on the microtubules shown in blue. Segregation of 3 μm (red) and 1 μm (green) spheres when cells are incubated (b) without nocodazole and (c) with 0.3 μM nocodazole for 6 h. Disruption of the microtubules leads to lack of particle segregation in the cells. Scale bar: 5 μm.

internalized by the cells are transported to the perinuclear region by microtubules. In the presence of the particles of varied sizes and shapes, the height of the cell and the height of the particle determine the position of the particle in the cell. The particles are separated based on the height regardless of the initial particle distribution. The likelihood of segregation is higher for a taller particle causing larger particles to be pushed towards the thicker regions of the cell. The smaller particles can coexist in the perinuclear region or pushed away from the nucleus depending on the number of the larger particles. This observation throws more light on the intracellular organization and importance of the size and shape of various organelles.

The study may also shed light into trafficking and intracellular localization of drug delivery carriers. Although particles as large as 3 μm are not routinely used for intravenous applications, they are used for subcutaneous injections for sustained release applications.[32–34] These particles are taken by immune cells and processed intracellularly through similar routes. The knowledge gained through the studies presented here sheds new light onto intracellular organization of these particles.

The segregation of bi-particle systems may also have implications for delivering drugs to the cytoplasm and the nucleus. Since the larger particles localize closer to the nucleus, a cargo encapsulated within them is likely to release closer to the nucleus than that encapsulated in smaller particles. This issue is particularly significant for the delivery of genes and RNA therapeutics. The exact location of release of gene or the siRNA into the cytoplasm has significant bearing on the therapeutic efficiency.[35] The probability of DNA delivery decreases exponentially with the distance from the nuclear membrane at which the DNA is released from the carrier. In case of siRNA delivery, it is also known that the knockdown depends greatly on the location of oligonucleotide release.[36] The segregation

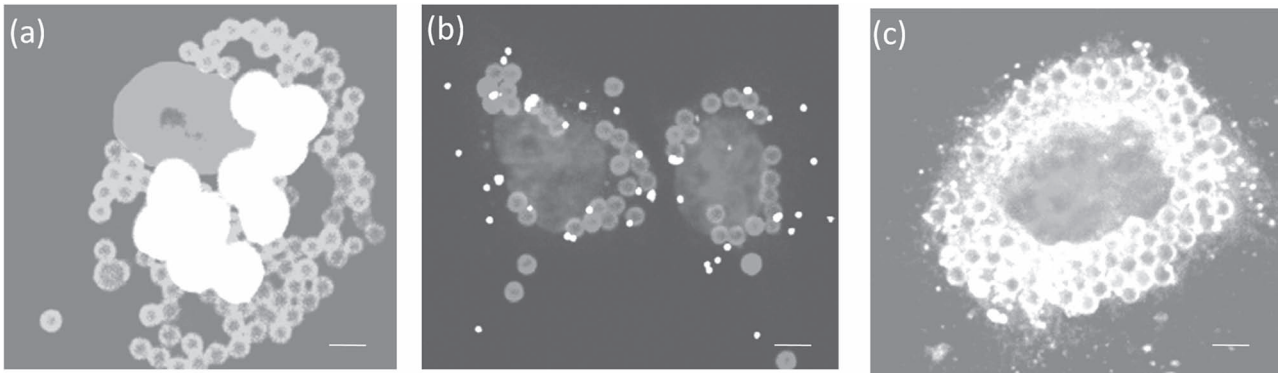

Figure 6. Threshold dimension of segregation: Confocal micrographs of cellular accumulation of (a) 3 μm spheres in red and 6 μm spheres in green (b) 3 μm spheres in red and 0.1 μm spheres in green, (c) 3 μm spheres in red and 0.1 μm spheres in green Scale bar: 5 μm.

of particles based on their size and shape can be potentially used to design carriers and strategies for efficient intracellular delivery into the cytoplasm or the nucleus.

Acknowledgements

P.K. acknowledges a fellowship from California Institute of Regenerative Medicine.

Received: December 1, 2011
Revised: February 3, 2012
Published online: May 23, 2012

[1] F. S. Sjostrand, *Nature* **1953**, *171*, 30.
[2] C. Pangarkar, A. T. Dinh, S. Mitragotri, *Phys. Rev. Lett.* **2005**, *95*, 158101.
[3] S. L. Rogers, V. I. Gelfand, *Curr. Opin. Cell Biol.* **2000**, *12*, 57.
[4] R. D. Vale, *Annu. Rev. Cell Biol.* **1987**, *3*, 347.
[5] L. M. Bareford, P. W. Swaan, *Adv. Drug Delivery Rev.* **2007**, *59*, 748.
[6] P. Watson, A. T. Jones, D. J. Stephens, *Adv. Drug Delivery Rev* **2005**, *57*, 43.
[7] J. Suh, D. Wirtz, J. Hanes, *Biotechnol. Prog.* **2004**, *20*, 598.
[8] A. Rustom, R. Saffrich, I. Markovic, P. Walther, H. H. Gerdes, *Science* **2004**, *303*, 1007.
[9] S. L. Rogers, V. I. Gelfand, *Curr. Biol.* **1998**, *8*, 161.
[10] M. Zerial, H. McBride, *Nat. Rev. Mol. Cell Biol.* **2001**, *2*, 107.
[11] M. Versaevel, T. Grevesse, S. Gabriele, *Nat. Commun.* **2012**, *3*, 671.
[12] R. D. Deegan, O. Bakajin, T. F. Dupont, G. Huber, S. R. Nagel, T. A. Witten, *Phys. Rev. E Stat. Phys. Plasmas Fluids Relat. Interdiscip. Topics* **2000**, *62*, 756.
[13] X. Jia, M. Gan, R. A. Williams, D. Rhodes, *Powder Technol.* **2007**, *174*, 10.
[14] M. Schena, D. Shalon, R. W. Davis, P. O. Brown, *Science* **1995**, *270*, 467.
[15] H. Sirringhaus, T. Kawase, R. H. Friend, T. Shimoda, M. Inbasekaran, W. Wu, E. P. Woo, *Science* **2000**, *290*, 2123.
[16] E. Garcia-Garcia, K. Andrieux, S. Gil, H. R. Kim, T. Le Doan, D. Desmaele, J. d'Angelo, F. Taran, D. Georgin, P. Couvreur, *Int. J. Pharm.* **2005**, *298*, 310.
[17] J. W. Yoo, N. Doshi, S. Mitragotri, *Macromol. Rapid. Commun.* **2010**, *31*, 142.
[18] J. Rejman, V. Oberle, I. S. Zuhorn, D. Hoekstra, *Biochem. J.* **2004**, *377*, 159.
[19] S. E. Gratton, P. A. Ropp, P. D. Pohlhaus, J. C. Luft, V. J. Madden, M. E. Napier, J. M. DeSimone, *Proc. Natl. Acad. Sci. USA* **2008**, *105*, 11613.
[20] S. Mishra, P. Webster, M. E. Davis, *Eur. J. Cell Biol.* **2004**, *83*, 97.
[21] S. K. Lai, K. Hida, S. T. Man, C. Chen, C. Machamer, T. A. Schroer, J. Hanes, *Biomaterials* **2007**, *28*, 2876.
[22] V. K. Kodali, W. Roos, J. P. Spatz, J. E. Curtis, *Soft Matter* **2007**, *3*, 337.
[23] J. A. Champion, S. Mitragotri, *Proc. Natl. Acad. Sci. USA* **2006**, *103*, 4930.
[24] J. A. Champion, S. Mitragotri, *Pharm. Res.* **2009**, *26*, 244.
[25] Y. Geng, P. Dalhaimer, S. Cai, R. Tsai, M. Tewari, T. Minko, D. E. Discher, *Nat. Nanotechnol.* **2007**, *2*, 249.
[26] P. Decuzzi, R. Pasqualini, W. Arap, M. Ferrari, *Pharm. Res.* **2009**, *26*, 235.
[27] E. Ruoslahti, S. N. Bhatia, M. J. Sailor, *J. Cell Biol.* **2010**, *188*, 759.
[28] J. A. Champion, Y. K. Katare, S. Mitragotri, *Proc. Natl. Acad. Sci. USA* **2007**, *104*, 11901.
[29] J. W. Yoo, S. Mitragotri, *Proc. Natl. Acad. Sci. USA* **2010**, *107*, 11205.
[30] X. Jia, R. Caulkin, R. A. Williams, Z. Y. Zhou, A. B. Yu, *Epl-Europhys. Lett.* **2010**, 92.
[31] R. Caulkin, X. Jia, M. Fairweather, R. A. Williams, *Phys. Rev. E* **2010**, 81.
[32] Y. Ogawa, H. Okada, T. Heya, T. Shimamoto, *J. Pharm. Pharmacol.* **1989**, *41*, 439.
[33] T. Uchida, S. Martin, T. P. Foster, R. C. Wardley, S. Grimm, *Pharm. Res.* **1994**, *11*, 1009.
[34] T. Uchida, S. Goto, T. P. Foster, *J. Pharm. Pharmacol.* **1995**, *47*, 556.
[35] A. T. Dinh, C. Pangarkar, T. Theofanous, S. Mitragotri, *Biophys. J.* **2007**, *92*, 831.
[36] W. Gao, Z. Xiao, A. Radovic-Moreno, J. Shi, R. Langer, O. C. Farokhzad, *Methods Mol. Biol.* **2010**, *629*, 53.